Proceedings of ISFOG 2025
5TH INTERNATIONAL SYMPOSIUM ON
FRONTIERS IN OFFSHORE GEOTECHNICS
Nantes, France | June 9-13 2025

ISBN 978-2-85782-758-0

Boulder damage during monopile installation through strong clay: initiation and growth

M. F. Randolph, J. Nietiedt, F. da Silva Pereira, B. Bienen*, L. Feske
Centre for Offshore Foundation Systems, University of Western Australia, Perth, Australia

C. Tejada
Ørsted, London, United Kingdom

J. de Sordi
Equinor, Stavanger, Norway

britta.bienen@uwa.edu.au (corresponding author)

ABSTRACT: The presence of sizable boulders can be established with some confidence from high resolution geophysical surveys. The important question that remains is: Will a boulder of a given size damage the monopile during installation and will minor tip damage then grow? Depending on the set of conditions, the boulder may simply be moved out of the path of the advancing monopile. At the other extreme of the potential outcomes is a severely damaged monopile that may not be possible to install to target depth, let alone provide a safe and reliable foundation for the offshore wind turbine. This contribution draws on evidence from centrifuge model testing and numerical modelling to inform a framework originally established for dense sand conditions to evaluate the potential and expected severity of damage in a different soil type.

Keywords: Pile; installation; boulder; tip damage; extrusion buckling

1 INTRODUCTION

Large diameter, thin-walled piles, such as monopiles that support the majority of bottom-fixed offshore wind turbines, are susceptible to distortion at the pile tip, particularly when driven into strong sediments or interacting with a boulder.

Pile tip damage may often go undetected, especially when mild, as the resulting change in the driving resistance may not be obvious.

Figure 1. Pile tip damage (Broos et al. 2017)

An example of pile tip damage that went unnoticed during the installation is shown in Figure 1 (Broos et al. 2017). The piles were 1.42 m in diameter D and had a wall thickness t = 17 mm, i.e. D/t = 84. The piles were installed at a rake of 1 in 5, such that any stronger soil layer would have been encountered unevenly over the pile tip. The rake is likely to have contributed to the tip damage, which was discovered when the piles were extracted during widening of the Rotterdam harbour basin.

This has relevance for monopiles where the D/t may be of the order of 100. Monopiles may encounter sloping strong layers or boulders located within the soil matrix, which apply pressure unevenly across the pile annulus as shown schematically in Figure 2.

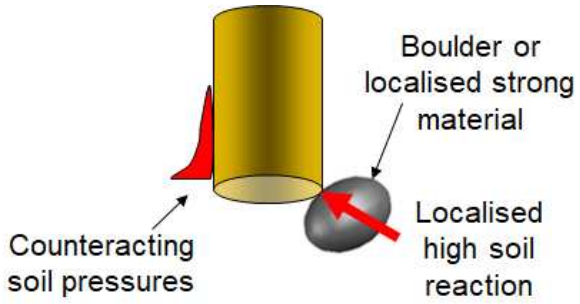

Figure 2. Initiation of pile tip damage through boulder interaction (schematic)

The consequences range from the boulder being displaced by the advancing pile (with little to no damage to the pile) to severe tip damage (tip closure),

potentially preventing pile installation to target depth and compromising performance of the offshore wind turbine foundation. Hence, a priori evaluation of potential pile tip damage from boulder interaction is required during offshore wind farm planning.

Initial minor tip damage or ovalisation of the pile may grow through extrusion buckling as pile driving continues. The soil must be sufficiently stiff to overcome the elastic hoop stiffness of the steel pile. The risk therefore increases with increasing D/t.

API (2011) includes a guideline that is often used as the basis for selecting the pile wall thickness at the tip. However, it targets a different form of pile tip damage linked to the generation of excessive axial stresses during installation by driving and therefore should not be used to evaluate potential tip damage from asymmetric lateral pressure near the tip or the gradual distortion that occurs in extrusion buckling.

A framework to assess likely pile tip damage and the risk of extrusion buckling was developed for piles being driven into sand (Nietiedt et al. 2023d) on the basis of structural and geotechnical considerations, with evidence from large deformation numerical modelling and physical modelling in the centrifuge. The framework, couched in non-dimensional terms, was compared to dynamically installed large scale pile-boulder interaction field tests performed in sand, showing good agreement (Balscheit et al., 2024).This paper applies the framework to monopiles being driven into strong clay containing boulders and evaluates the predictions against the results from 21 centrifuge tests and 36 large deformation numerical analyses.

2 FRAMEWORK FOR DENSE SAND

A framework to evaluate damage due to boulder impact on open-ended driven piles has been developed for sand in Nietiedt (2022), Nietiedt et al. (2023a-d). In the evaluation, the structural resistance of the pile to a concentrated force F_p (i.e. the force required to initiate a dent) is compared with the maximum lateral force $R_{h,max}$ that a boulder embedded in a given soil matrix might exert on the pile. This was found to be directly proportional to the cone tip resistance q_c and the plan area of the boulder. It is assumed throughout that the boulder would not split.

Minor pile tip damage such as localised indentation may not, of itself, affect the drivability very much. However, if the sediments through which the pile is driven are sufficiently strong, minor damage is likely to grow in a process referred to as extrusion buckling. Growth of the initial damage may lead to much more significant driving resistance and even full closure and plastic crumpling of the pile.

Firstly, the force to cause further plasticity is estimated starting from different initial dent magnitudes. Then, soil reactions generated as the angled dent penetrates soil are quantified. Design charts showing the likelihood of dent growth (extrusion buckling) as a function of soil strength (i.e. cone resistance q_c) have been established.

3 MONOPILE-BOULDER INTERACTION IN A HARD CLAY MATRIX

Evidence of monopile-boulder interaction in strong clay was obtained from a combination of large deformation numerical analyses and physical modelling in the centrifuge.

3.1 Centrifuge experiments

The centrifuge experiments were performed at 80g in the 10 m diameter beam centrifuge in the National Geotechnical Centrifuge Facility (NGCF) at the University of Western Australia, where the previous tests in sand were carried out as well (Nietiedt 2022, Nietiedt et al. 2020, 2023b).

3.1.1 Sample Preparation

To produce samples with strength comparable with strong clay found offshore, a process involving cement addition and consolidation was adopted. The properties of the kaolin clay are summarised in Wang et al. (2023). High early strength cement compliant with AS 3972 (2010) was used. Blue metal aggregate as used by Nietiedt et al. (2023b), with diameter of 10 - 15 mm (20 to 30% of the model pile diameter), equivalent to 0.8 m to 1.2 m in prototype scale, was used to model the boulders (Figure 3). The unconfined compressive strength of the source rock is usually around 100 – 250 MPa.

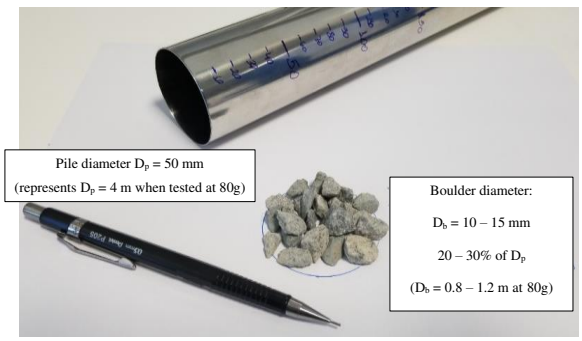

Figure 3. Model boulders relative to model pile

Two samples were produced following the same process. Initially, 80 % of the total water volume was mixed with the kaolin and allowed to hydrate for one hour. The cement was then diluted in the remaining 20% of water in small batches inside a plastic container and added to the mix. At least 20 minutes of mixing was allowed to obtain a uniform mixture. The cement to dry kaolin ratio (cement content) was 15% for Sample A and 18% for Sample B. The initial water content of the clay-cement mix was ~ 140 %.

The samples were prepared in a 'strongbox' container measuring 1 m × 1 m × 0.5 m. A drainage layer composed of gravel with a geotextile on top, was placed at the base of the strongbox to allow for two-way drainage during sample consolidation. Sufficient clay-cement mix was then placed inside the strongbox to result in at least 140 mm of consolidated mix. Then, the boulder layer with a thickness of one boulder was placed. At each pile testing site, the model boulders were spaced such that they acted independently rather than be influenced by each other and that the penetrating pile was likely to hit at least one boulder. With this arrangement, the pile would contact the boulder(s) at one or more locations on the pile tip annulus, inducing some degree of damage at the tip. Locations between the boulder patches were left across the box for cone penetrometer and reference pile tests (Figure 4).

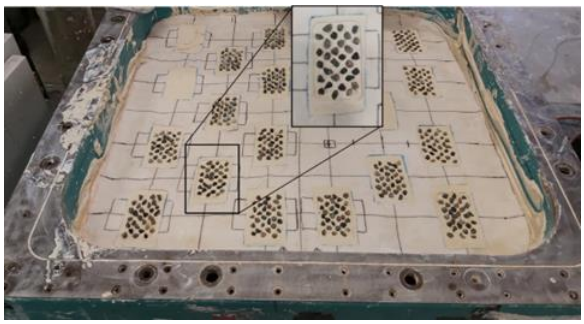

Figure 4. Boulder layer placement, sample preparation

A final layer of clay-cement mix was placed on top of the boulder layer, targeted to yield a consolidated thickness of ~70 mm (targeted boulder layer depth). The samples were then moved to the hydraulic press where the consolidation pressure was increased in steps. The sample was allowed to consolidate and cure for at least 7 days in the press, albeit no significant consolidation was observed after 5 (sample A) and 9 (sample B) hours, reflecting the cement settling and hence increased sample stiffness. The maximum consolidation pressure was 300 kPa and 420 kPa for Sample A and Sample B, respectively.

Several cone penetration tests were performed in-flight in both samples, with the measured cone penetration resistance presented on Figure 5. At the boulder depth of 5-6 m, the cone penetration resistance ranged from 3 to 3.5 MPa in sample A, and from 3.8 to 5 MPa in sample B.

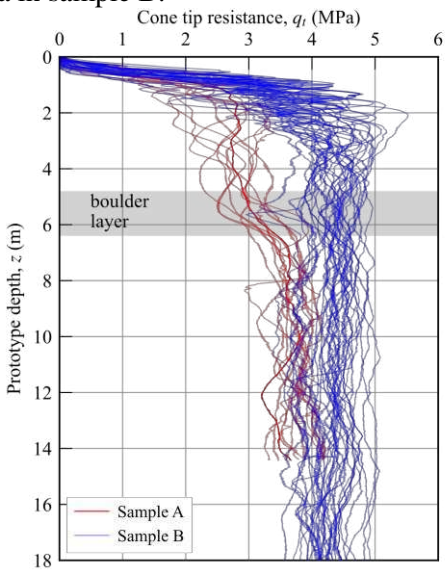

Figure 5. Cone tip resistance for Sample A and Sample B

3.1.2 Model Piles

The model piles comprised 0.5 m lengths of stainless-steel tubing. The external diameter of 50 mm, represented a 4 m diameter prototype pile when tested at 80g. The average wall thickness for the piles with $D/t = 100$ was 0.51 mm, while it was 1 mm for the piles with $D/t = 50$. Slight out of circularity, $(D_{max} - D_{min})/D_{nominal}$ of 0.4 to 1.2%, of the piles was measured, but the piles were found to be closely parallel relative to a central axis. The manufacturers quote the material as a V2A-steel, with yield stress of 205 MPa, Young's modulus of 207 GPa and density of 7.8 Mg/m^3.

3.1.3 Pile Driving Set-up and Instrumentation

The pile driving set-up developed previously at COFS (Nietiedt et al. 2023e) was utilised, although with a slightly simplified arrangement. The pile itself was attached to a 'follower', 150 mm long with wall thickness of 2 mm. The top of the follower has a 10 mm thick cap with a central threaded hole into which is screwed a solid 'button', 10 mm diameter but with a wider (13.5 mm) head. An anvil rests on the pile button during driving but is shaped like a claw that can hook under the top wider section of the pile button in order to lift the pile. During driving, the anvil is impacted by the 12 mm diameter ram of the hammer. For further details on the experimental set-up see Nietiedt et al. (2023e).

3.1.4 Experimental Programme

The experimental program covers a large scope, and only selected results are presented in this paper. The

drop height, hence hammer energy, was gradually increased as required as indicated in the results figures.

Table 1. Testing programme.

Sample	Test	D/t	Boulder
	A_PF2	100	no
A	A_PB3	100	yes
	B_PF1	100	no
	B_PB1	100	yes
	B_PB2	100	yes
	B_PF2	50	no
	B_PB7	50	yes
B	B_PB8	50	yes

3.1.5 Experimental Results

For the three pile tests in which the pile did not make contact with boulders but was driven through clay only (A_PF2, B_PF1 and B_PF2), the pile driving resulted in minor changes in circularity (see photos in Figure 6 and 7), particularly for the pile with D/t = 50 (B_PF2). The pile driven in Sample A at a location with boulders (A_PB3), sensed the boulders at ~5.1 m depth, when a marked increase in the blowcount was observed (Figure 6, inset). The pile was significantly distorted, despite the blow count number at end of installation being similar to the pile installed in the bolder free region (A_PF2).

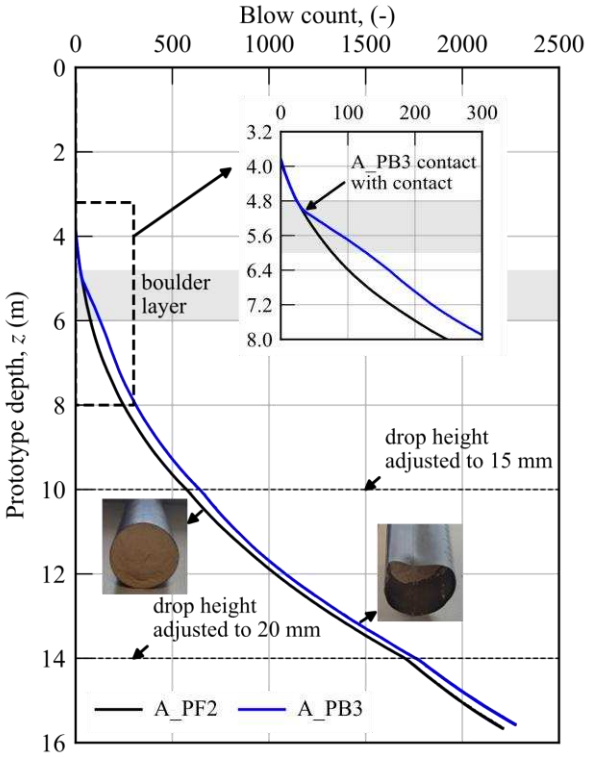

Figure 6. Blow count for selected tests in Sample A

The two piles with *D/t* = 100 were installed at locations with boulders in Sample B, with boulder being sensed at ~5.5 m and ~5.9 m for piles B_PB1 and B_PB2, respectively (see Figure 7, inset). Both piles were severely distorted during installation. By contrast, the piles with *D/t* = 50 installed in the boulder region (B_BP7 and B_PB8) only experienced slight increase in out of circularity, despite the boulder being clearly sensed at ~5.5 m (B_PB7) and ~6.0 m (B_PB8) (Figure 7, inset).

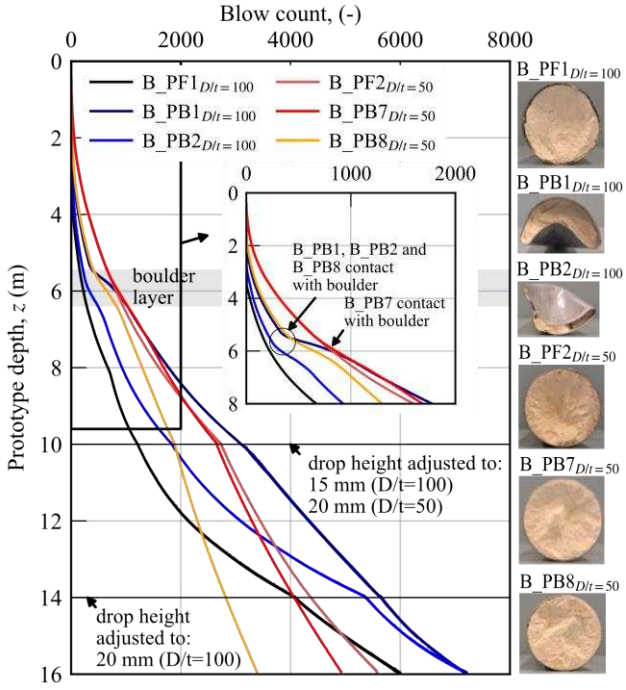

Figure 7. Blow count for selected tests in Sample B

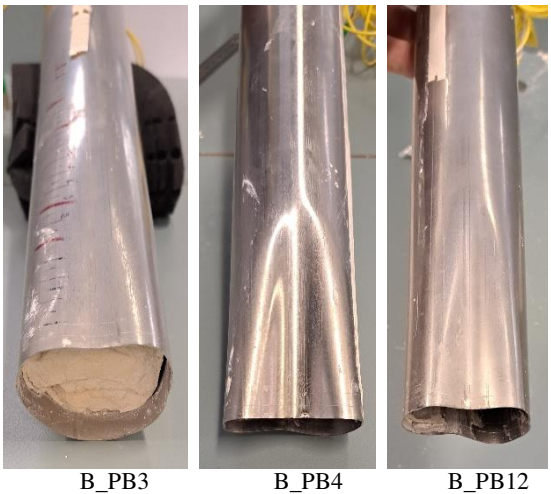

Figure 8. Pile shapes for selected tests in Sample B

In addition to tip damage arising from the boulder impact, damage growth due to extrusion buckling was observed for almost all of the *D/t = 100* piles tested at boulder locations. Figure 8 shows examples from three of such tests.

3.2 Numerical modelling

The scope of numerical analyses comprised cone penetrometer tests, 28 simplified boulder-soil

interaction (which do not feature the pile explicitly and allow faster parametric studies) and 5 full pile-soil-boulder interaction analyses (modelling the pile penetration inclusive of boulder interaction, see Nietiedt et al. 2023a), all performed in Abaqus/CEL (version 2020) due to its large deformation modelling capabilities.

The soil was modelled using the Drucker-Prager option available in Abaqus, which when used with cohesion only is appropriate for modelling the undrained behaviour under consideration (with undrained shear strength s_u of up to 800 kPa modelled) and represents a robust and computationally efficient choice. Interactions between pile, soil and boulder for both simplified and full models were characterised as rough, though numerically forcing the cohesion of 100 kPa together with the high friction ratio of 0.95 (applied to total normal stress in Abaqus).

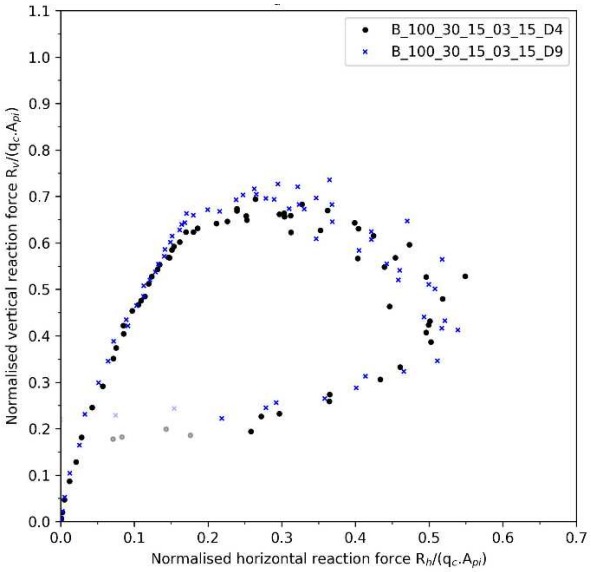

Figure 9. Normalised reaction forces of simulations with a/b-ratio = 1.5, s_u = 800 kPa

The boulder-soil analyses simplified the problem to interaction of the boulder and soil, to extract the force required to displace the boulder. The boulder was modelled as an ellipsoid of width a_b and height b_b. Different sizes were modelled. The loading point was at an eccentricity e relative to the vertical axis of symmetry of the boulder. The boulder was wished-in-place and modelled as a rigid body, neglecting deformation of the boulder itself and the possibility of breakage. The boulder was displaced by applying a vertical velocity of 5 m/s at the reference point (which is offset from the boulder centreline by the eccentricity), allowing rotation of the boulder but no horizontal displacement of the reference point. This yielded curves of normalised vertical (R_v) and horizontal (R_h) reaction forces (like in Nietiedt et al. 2023a), examples of which are shown in Figure 9. The normalisation is done in terms of the cone tip resistance q_c at (mid) embedment depth and A_{pi} is the projected area of the boulder ellipsoid.

In the full pile-soil-boulder interaction analyses, the pile is penetrated from the soil surface to interact with a boulder that is wished-in-place at a depth of 1.5D and a pre-defined location (or eccentricity) with respect to the path of the pile wall. The pile penetration velocity in the numerical model was set to 10 m/s. Figure 10 shows an example result.

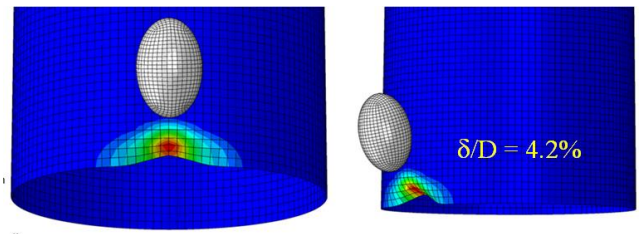

Figure 10. Pile tip damage (numerical result) from a boulder of a_b = 1.2 m, b_b = 0.8 m, e = 0.1a_b, q_c ~ 1.7 MPa, D/t = 100

4 DISCUSSION

The physical and numerical modelling results cover pile tip damage from negligible to severe, with the data further interpreted in the framework proposed by Nietiedt et al. (2023d).

Considering first piles with D/t = 100, the relationship for the force F_p to cause a dent in the pile, F_p varies from 0.14 MN to 0.17 MN as the loaded length s_{load} that is being considered increases from 0.16 m to 0.24 m. Nietiedt et al. (2023d) recommended taking s_{load} as 20% of the boulder diameter, hence the range of s_{load} quoted above corresponds to boulder diameters of 0.8 m to 1.2 m. The maximum horizontal reaction $R_{h,max}$ due to impact with a boulder is proportional to the cone resistance and the projected area of the boulder (so a_b^2).

In the model tests the cone resistance at the boulder depth ranged between 3 and 3.5 MPa in Sample A, and 3.8 and 4.8 MPa in Sample B. For the CEL analyses cone resistances were 1.7, 3.8 and 5.8 MPa. This gives $R_{h,max}/q_cA_{pi}$ in the range 0.30 to 0.41 and corresponding ratios $R_{h,max}/F_p$ in the range 1.4 to 7.0 for the relevant ranges of experimental and numerical cone resistances and prototype boulder diameters. As such, any boulder impact is likely to initiate a medium to severe dent, with δ/D of at least 1%, which is consistent with the quite severe denting observed experimentally. This magnitude of dent compares with the value to initiate plasticity of δ_p/D of approximately 0.3%.

For thicker-walled piles with D/t = 50, the resulting reaction ratios $R_{h,max}/F_p$ exceed unity for the largest

boulder size except for the weakest soil, while for the smallest boulder size it remains below unity until the cone resistance reaches 3.8 MPa. For the soil conditions in centrifuge Sample B, in which the thicker-walled piles were tested, the cone resistance was in the range 3.8 to 4.8 MPa and the reaction ratio is between 1.0 (smallest boulder) and 1.9 (largest boulder). This is slightly at odds with the experimental results, which showed essentially no tip damage for the thicker-walled piles. The reasons for this discrepancy are not apparent.

Applying the Nietiedt et al. (2023d) framework for extrusion buckling, for the relevant conditions the framework suggests that damage growth should not have occurred in the cemented clay samples, taking account of the lower cone tip resistances compared with those in dense sand for which the framework was developed. While the lack of damage growth is consistent with the numerical analyses, where no significant growth in the initial dent was observed, it appears inconsistent with the quite extensive damage growth observed in the majority of the thinner-walled piles tested experimentally.

5 CONCLUSIONS

During monopile installation for offshore wind farms, boulders may be encountered. This paper has addressed the questions: Will a boulder of a given size damage the monopile during installation and will minor tip damage then grow?

Data from the physical and numerical modelling of monopile-boulder interaction in clay were evaluated using a framework (Nietiedt et al. 2023d) couched in non-dimensional terms that was previously developed for piles in sand. The pile tip damage observed in physical centrifuge tests of D/t = 100 piles is consistent with damage expected from using the Nietiedt framework; however, the framework overestimates the damage in D/t = 50 piles where negligible damage was observed in the centrifuge tests. This apparent conservatism may be a function of the different soil conditions (cemented clay, compared with dense sand). The Nietiedt framework for dent growth by extrusion buckling suggests that this should not occur for the magnitudes of cone resistance measured in the tests. Although this is consistent with the numerical analyses, it is at odds with the marked distortion observed in almost all of the D/t = 100 model tests. It appears that the damage growth framework needs to evolve in the light of new data covering a wider variety of soil types.

AUTHOR CONTRIBUTION STATEMENT

M.F. Randolph: Conceptualization, Methodology, Validation, Writing – review & editing. **J. Nietiedt**: Methodology, Writing – review & editing. **F. da Silva pereira**: Data Curation, Formal analysis, Visualization, Writing – review & editing. **B. Bienen**: Conceptualization, Methodology, Project administration, Supervision, Writing- Original draft. **L. Feske**: Data Curation, Formal analysis, Visualization. **C. Tejada, J. De Sordi**: Project initiation, technical discussions, Writing – review & editing

REFERENCES

API (2011). *Recommended Practice 2GEO Geotechnical and Foundation Design considerations*, 1st edition, American Petroleum Institute, Washington.

Balscheit, H., Geißler, P., Cuéllar, P., Basedau, F. and Baeßler, M. (2024). Large-scale field tests on plastic pile tip failure upon monopile installation. *Ocean Engineering*, 313, p.119322, https://doi.org/10.1016/j.oceaneng.2024.119322.

Broos, E., Sibbes, R., de Gijt, J. (2017). Widening a harbor basin, demolition of a deep sea quay wall in Rotterdam. *Proc. COME2017: Decommissioning of Offshore Geotechnical Structures*, Hamburg, Germany, pp. 251-262.

Nietiedt, J. (2022). *Pile tip damage and extrusion buckling assessment through centrifuge modelling and large deformation finite element analysis*. PhD Thesis, The University of Western Australia.

Nietiedt, J., Randolph, M.F., Gaudin, C., Doherty, J.P., Kallehave, D., Gengenbach, J. and Shonberg, A. (2020). Physical modelling of pile tip damage arising from impact driving. *Proc. 4th Int. Symp. on Frontiers in Offshore Geotechnics, ISFOG2020,* Austin, USA, 787-797.

Nietiedt, J., Randolph, M.F., Gaudin, C. and Doherty, J.P. (2023a). Numerical assessment of tip damage during pile installation in boulder rich soils. *Géotechnique*, doi: 10.1680/jgeot.21.00395.

Nietiedt J.A. Randolph M.F. Doherty J.P. Gaudin C. (2023b). Centrifuge model tests investigating initiation and propagation of pile tip damage during driving. *J. Geot. Geoenv. Eng. (ASCE)*, 149(5), 04023024.

Nietiedt J.A. Randolph M.F. Doherty J.P. Gaudin C. (2023c). Estimating initiation conditions for extrusion buckling of driven open-ended piles. *Géotechnique*, Vol. 74, No. 12, pp. 1431-1444, https:doi.org/10.1680/jgeot.22.00065.

Nietiedt, J.A., Randolph, M.F., Gaudin, C. and Doherty, J.P. (2023d). Preliminary assessment of potential pile tip damage and extrusion bucking. *Ocean Engineering*, 275, 114071.

Nietiedt, J.A., Randolph, M.F., Gaudin, C. and Doherty, J.P. (2023e). Development of a high-energy centrifuge model impact hammer for pile-driving. *International Journal of Physical Modelling in Geotechnics*, 24(2), 56-65.